Weakly coupled antiferromagnetic planes in single-crystal $LiCoPO_4$

D. Vaknin,[1] J. L. Zarestky,[1] L. L. Miller,[1] J.-P. Rivera,[2] and H. Schmid[2]
[1]*Ames Laboratory and Department of Physics and Astronomy, Iowa State University, Ames, Iowa 50011*
[2]*Department of Inorganic, Analytical and Applied Chemistry, University of Geneva, Sciences II, 30 quai E. Ansermet, CH-1211-Geneva 4, Switzerland*
(Received 21 December 2001; published 30 May 2002)

Neutron-scattering and magnetic susceptibility studies of single-crystal $LiCoPO_4$ are reported. The neutron-diffraction results indicate that in the antiferromagnetic phase the moments are not strictly aligned along the *b* axis, as previously reported [R. P. Santoro *et al.*, J. Phys. Chem. **27**, 1192 (1996)], but are uniformly rotated from this axis by a small angle ($\approx 4.6°$). This rotation breaks the mirror symmetry along the orthorhombic *b* axis. Symmetry considerations based on this rotation, on the magnetoelectric effect, and on a recently observed weak spontaneous magnetization along the spin direction, implying a so-far-unknown ferrimagneticlike kind of weak ferromagnetism, allow one to postulate the monoclinic magnetic point group $2'$. The diffraction data are analyzed in terms of weakly coupled two-dimensional Ising antiferromagnets. The large anisotropy in the susceptibility is explained in terms of the single-ion anisotropy and anisotropic exchange interactions. We argue that the alignment of the magnetic moments in the antiferromagnetic phase is determined by the single-ion anisotropy even though the exchange along this direction is the weakest.

DOI: 10.1103/PhysRevB.65.224414 PACS number(s): 75.25.+z, 75.50.Ee, 78.20.Ls

I. INTRODUCTION

$LiCoPO_4$ belongs to a class of materials that exhibit properties intermediate to two- and three-dimensional (2D and 3D) systems. It consists of buckled CoO layers that are stacked along the crystallographic *a* axis. Nearest neighbors in the plane are coupled magnetically by a relatively strong superexchange interaction through an *M*-*O*-*M* oxygen bond[1–4] which with the influence of crystal field, renders an Ising-like character to the exchange interaction. There is no direct or indirect exchange coupling between the Co^{2+} moments ($S=3/2$) in different planes, and only higher-order exchange interaction involving the phosphate group is possible via Co-O-P-O-Co, as suggested by Mays.[1] The *M*-O-P-O-*M* (*M*=transition metal ion) is the only superexchange in some related 3D frameworks, such as $Li_3Fe_2(PO_4)_3$, where the 3D antiferromagnetic (AF) ordering occurs at relatively large temperatures.[5] This suggests that this type of magnetic coupling, although of a higher order, is not negligible. Crystal-field effects, in these systems, play an important role in reducing the spin symmetry of the magnetic moments. In particular, the orthorhombic symmetry introduces crystal-field terms that give rise to doublet ground state.

$LiCoPO_4$ is an insulator that is isostructural with the olivine family of lithium orthophosphates $LiMPO_4$ (*M*=Mn, Fe, Co, and Ni),[6] space group *Pnma* with lattice constants $a=10.093$ Å, $b=5.890$ Å, and $c=4.705$ Å at room temperature. It consists of two types of polyhedra: CoO_6 octahedra that are corner shared and cross-linked with the PO_4 tetrahedra, forming a three dimensional network, with tunnels that are occupied by Li ions along the [010] and [001] directions. In this network, nearly close-packed oxygens in hexagons can be found. Interest in inorganic Li phosphates for potential rechargeable batteries has risen recently.[7] According to Ref. 3, $LiCoPO_4$ undergoes an antiferromagnetic phase transition with a colinear arrangement of the Co^{2+} spins, as shown in Fig. 1. The in-plane spin configuration with a propagation vector along the (010) is similar in all $LiMPO_4$ members, and differs only in spin orientation from one member to another. In $LiCoPO_4$ the spin direction was found to be along the *b* axis.[2] However, recent magnetoelectric effect (ME) and magnetic susceptibility studies of $LiCoPO_4$ by Rivera[8,9] indicated strong anisotropic properties, and suggested that the spin configuration might be of a lower symmetry than the one shown in Fig. 1. We have undertaken this study to determine the detailed magnetic arrangement of $LiCoPO_4$ in a single crystal and to characterize the behavior of the magnetic system at low temperatures.

II. EXPERIMENTAL DETAILS

Neutron-scattering measurements were carried out on the HB1A triple axis spectrometer at the High Flux Isotope Reactor at Oak Ridge National Laboratory. A monochromatic neutron beam of wavelength $\lambda=2.358$ Å (14.712 meV and $k_o=2\pi/\lambda=2.653$ Å^{-1}) was selected by a double mono-

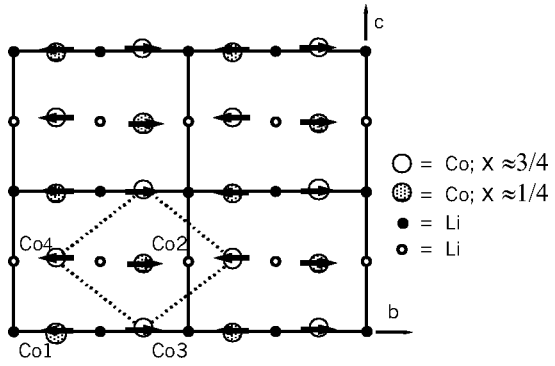

FIG. 1. Projection of $LiCoPO_4$ on the *b*-*c* plane, showing two layers of Co and Li atoms and the magnetic model as determined by Santoro *et al.* One layer of Co^{2+} is represented by open circles, and the adjacent layers in the *a* direction by filled circles.

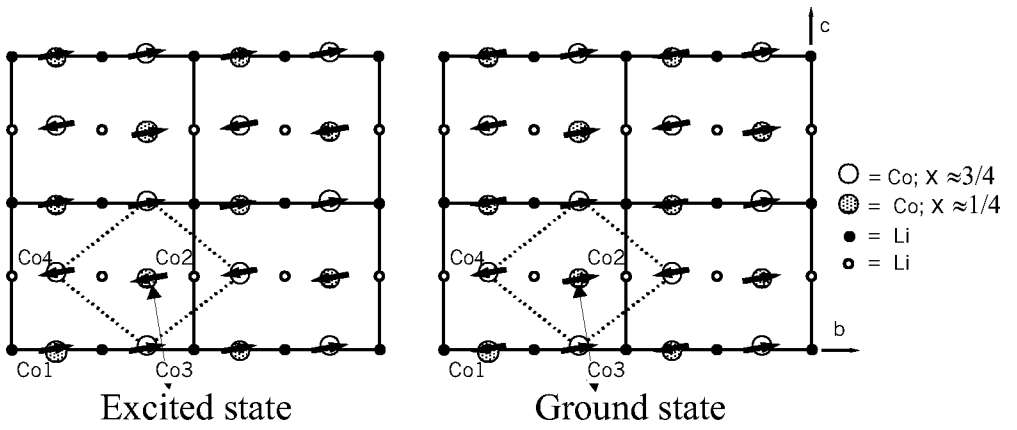

FIG. 2. The modified ground-state magnetic model of the present study. The magnetic moments are uniformly rotated by a small angle (4.6°, rotation is larger in the figure) around the *a* axis. The model is not unique; a rotation of the spins around the *c* axis is compatible with the observations. Each independent layer is degenerate with respect to the rotation of spins by 180°, however, the stacking of layers removes this degeneracy.

chromator system using the (002) Bragg reflection of highly oriented pyrolytic graphite (HOPG) crystals. The $\lambda/2$ component in the beam was removed (to better than 1.3 parts in 10^6) by a set of HOPG crystals situated between the two monochromating crystals. The collimating configuration 40′,40′, *Sample*, 34′,68′ was used throughout the experiments. Pyrolytic graphite was also used as the analyzer crystal. Temperature was controlled by a Conductus LTC-20 using Lake Shore silicon-diode temperature sensors (standard curve 10). The accuracy of the controller in reading the sensors is ± 0.01 K, and the accuracy of the sensors in the temperature range of the experiment is 0.5 K. However the repeatability of the sensors is 20 mK, allowing one to control and reproduce temperatures to better than ± 0.01 K. The sample was mounted on a thin aluminum post, sealed in an aluminum can under helium atmosphere and cooled using a closed-cycle He refrigerator (Displex). Temperature sensors were mounted in the cold tip of the Displex and at the top of the sample can above the neutron beam. The temperature difference between the two sensors was 0.2 K over the duration of the experiment and over the temperature range investigated.

III. RESULTS AND DISCUSSION

A. Neutron scattering

1. Diffraction

The AF spin arrangement of $LiCoPO_4$ used by Santoro *et al.*[3] is shown in Fig. 1, with Co^{2+} ($S=3/2$) ions located at $[\frac{1}{4}+\epsilon,\frac{1}{4},-\delta]$,$[\frac{1}{4}-\epsilon,\frac{1}{4},\frac{1}{2}-\delta]$ (labeled Co1 and Co2) anti-parallel to one another and the ions at $[\bar{\frac{1}{4}}-\epsilon,\bar{\frac{1}{4}},\delta]$, $[\bar{\frac{1}{4}}+\epsilon,\frac{1}{4},\frac{1}{2}+\delta]$ (Co3 and Co4) anti-parallel to the first pair. Here $\epsilon=0.0286$ and $\delta=0.0207$.[10] Our diffraction study confirms the main features of the magnetic arrangement of $LiCoPO_4$. However, in addition to the strong magnetic reflections compatible with the colinear magnetic model shown in Fig. 1, we observe a very weak peak at the (010) reflection which is forbidden by this spin arrangement. This observation indicates that the ordered moment is not strictly oriented along the *b* axis as determined from the powder diffraction study of Santoro *et al.*,[3] and that it has a small component oriented away from the *b* axis. The dimensionless magnetic structure factor for a general (h,k,l) reflection (regardless of spin direction), can be readily calculated on the basis of the magnetic model shown in Fig. 1:

$$F_M=\begin{cases} 4\sin\left[\pi\left(2h\varepsilon+\dfrac{k}{2}-2l\delta\right)\right]\cos\left(\dfrac{\pi \mathrm{h}}{2}\right) & \text{even} \quad l \\ 4\cos\left[\pi\left(2h\varepsilon+\dfrac{k}{2}-2l\delta\right)\right]\sin\left(\dfrac{\pi \mathrm{h}}{2}\right) & \text{odd} \quad l. \end{cases} \tag{1}$$

The ratio between magnetic and nuclear contributions to the integrated intensities of Bragg reflection (I_M/I_{nuc}) was used to determine the average magnetic moment from

$$\mu=\sqrt{\frac{I_M}{I_{nuc}}\frac{|F_{nuc}|^2}{|F_M|^2}\frac{1}{f^2(\mathbf{Q})\sin^2\phi}}, \tag{2}$$

where $f(Q)$ is the magnetic form factor of Co^{2+} at momentum transfer $Q=2k_0\sin\theta$, and $\mu=g\sqrt{S(S+1)}$ is the average magnetic moment of Co^{2+}. The magnetic and nuclear structure factors are calculated from known parameters of $LiCoPO_4$, and ϕ is the angle between the scattering vector and the spin direction. In this procedure all geometrical corrections to the calculated nuclear and magnetic contributions cancel out. This analysis yields a spin arrangement that is consistent with the colinear model of all $LiMPO_4$, however due to the observation of the weak (010) reflection, it requires a small uniform rotation of the spins by a 4.6° angle away from the *b* axis, as shown schematically in Fig. 2. Using Eq. (2) we extract an average magnetic moment $\mu=4.2\mu_B$ and a *g* value of 2.17.

To determine the temperature dependence of the order parameter, i.e., the staggered magnetization, the (200) and

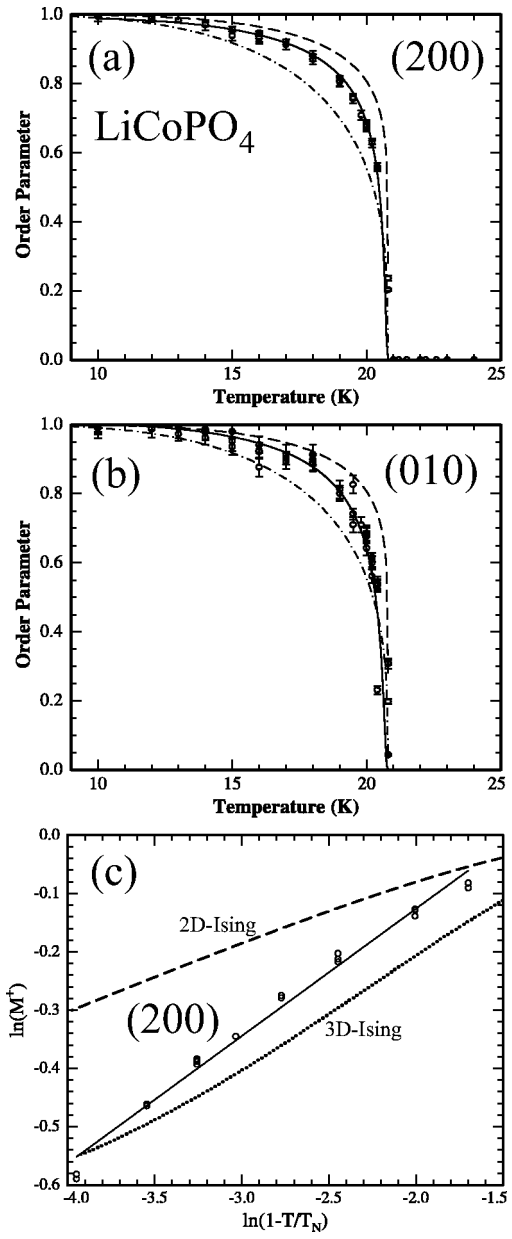

FIG. 3. (a) Temperature dependence of the order parameter as extracted from the magnetic contribution to the (200) reflection. The dashed line is calculated using the exact result for the 2D Ising model, the dash-dotted line is calculated by the series expansion [Essam and Fisher (Ref. 12)], and the solid line is from the 2D coupled-layer model as described in the text. (b) Same as (a), but for the (010) reflection from which it was deduced that the moments are slightly rotated from the *b* axis. (c) The temperature dependence of the order parameter close to the transition is showing a critical exponent $\beta \approx 0.218$.

the (010) reflections were monitored as functions of temperature. Figures 3(a) and 3(b) show the square root of the normalized integrated intensity which is proportional to the AF staggered magnetization $M^{\dagger}(T)$.

In qualitative terms we see that the uniform rotation of the moment from the *b* axis conforms to the main staggered magnetization, i.e., the small rotation of the spins from the *b* axis is practically the same at all temperatures. As a first step in the characterization of the spin system we analyze the order parameter in the vicinity of the transition. Figure 3(c) shows the measured ordered parameter near the critical point along with the calculated order parameter for the 2D Ising[11] and 3D Ising models,[12] suggesting that the dimensionality of the magnetic system is intermediate between the two. To construct a simplified spin Hamiltonian for the system we recall that the inplane superexchange interaction J_{2D} of nearest neighbors in $LiCoPO_4$ through the Co-O-Co path is expected to be much stronger than that between nearest interplane neighbors $J_{\perp}$ with a Co-O-P-O-Co path, which is of a higher-order perturbation.[1] Here we argue that the Ising-like behavior is invoked by a local perturbation term of the form $-D(S^z)^2$ due to crystal-field effects and spin-orbit coupling.[13] This term is common to transition-metal ions in an axial or rhombic symmetry[14] which, for Co^{2+}, leads to a zero-field splitting of the four magnetic levels into two doublets.

For $D>0$ the ground state of the spin system is doubly degenerate, and the only transformation that leaves the ground state invariant is the one in which $S^z \rightarrow -S^z$. According to the universality hypothesis,[15] the critical behavior of a spin system is dominated by the ground state of the free spin, and thus, by virtue of the zero-field-splitting term, the Co^{2+} spin system resembles that of the $S=\frac{1}{2}$ Ising model for which the spontaneous staggered magnetization is given by[11]

$$M_{2D}^{\dagger}(T) = M^{\dagger}(0)[1-\sinh^{-4}(2J_{2D}/T)]^{1/8}. \qquad (3)$$

The dashed lines in Fig. 3 are calculated with Eq. (3) whereas the dash-dotted lines are calculated by using the series expansion of Essam and Fisher[12] for the simple cubic system. Unlike some layered perovskites, such as K_2MF_4 (M=Co, Ni, Mn, Cu, and Fe) which behave as nearly perfect 2D systems,[16] the behavior of $LiCoPO_4$ is intermediate between the 2D and 3D systems. The interaction within the *bc* planes in $LiCoPO_4$ is uniform, where each spin is surrounded by four equidistant nearest neighbors. The coupling between spins in adjacent planes is much more complex and nonuniform. The eight out-of-plane nearest neighbors above and below each spin are located asymmetrically on two adjacent layers. Four of those are at 5.68, 5.3567, 6.36, and 6.36 Å, whereas the other four are at 5.68, 5.3567, 5.453, and 5.453 Å (this configuration alters within the plane depending on the position of the spin in the buckled layer). The differences in distances between nearest neighbors (NN's) in different planes give a slightly modified crystal field contribution, and small differences in the strength (if not the sign) of the exchange interaction. If all the interlayer NN exchange interactions were identical, the two ground states for stacking adjacent layers shown in Fig. 2 would be degenerate. The stacking of planes would be invariant to the rotation of spins in the plane with respect to those of a neighboring plane. If the exchange interactions are all ferromagnetic or all antiferromagnetic, then the two states are ''frustrated.'' However, due to the small differences in the neighborhood, we argue that the two states are at different energies. Thus, just below the onset of the 2D long-range order at T_N, the in-plane

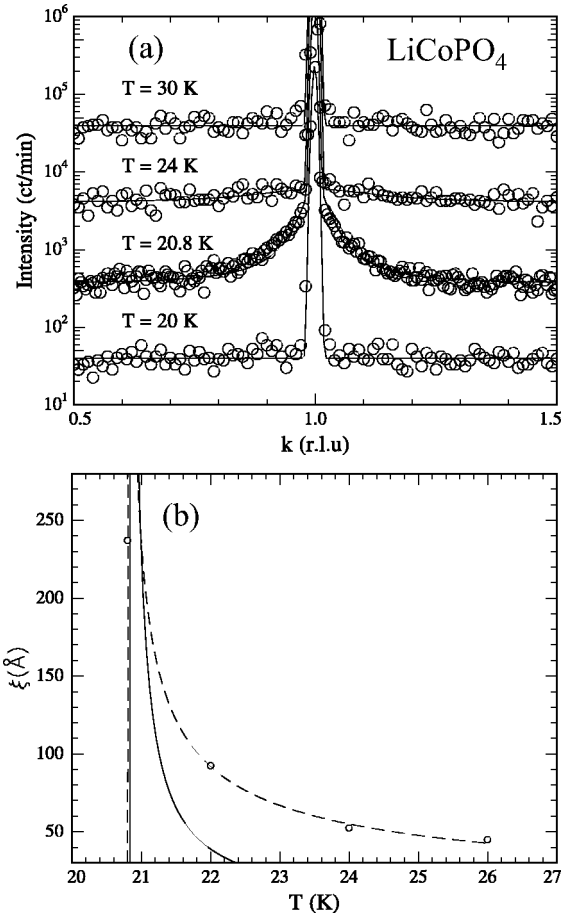

FIG. 4. (a) Critical scattering near T_N at the (210) reflection. (b) In-plane correlation length versus temperature; the solid line is the exact result for the 2D Ising model (see the text for more details), and the dashed line is a fit to the power law.

coherence length diverges in each plane. The in-plane ordering is invariant to flipping all spins by 180°; therefore, below the 3D ordering, there are two possibilities for the stacking of the planes as shown in Fig. 2. The two states are practically degenerate with respect to the exchange between nearest neighbors in adjacent layers (ferromagnetic or antiferromagnetic exchange) since the sum with the four NN's cancels out. The coupling between planes can now be characterized by two 2D macroscopic energies E_G and E_E (i.e., a two-state, Ising-like behavior) . With this in mind, the interlayer interaction of the staggered 2D magnetization can be approximated by the 1D Ising model. Although a 1D system does not order at any finite temperature, the magnetization at zero magnetic field and the correlation length grow exponentially as $M_{1D}\sim e^{2J_\perp/T}$ as the temperature is lowered. We therefore propose that the 1D fluctuations of the 2D ordered planes diverge exponentially at the transition temperature as $e^{|\Delta_{G-E}/(T-T_N)|}$, $\Delta_{G-E}\equiv E_G-E_E$, is the energy difference between the two states). Thus the crossover 3D magnetization (which is what the neutron diffraction measures) of coupled layers below T_N may be given by

$$M^{\dagger}_{CO}(T)\sim e^{|\Delta_{G-E}/(T-T_N)|}M^{\dagger}_{2D}(T). \qquad (4)$$

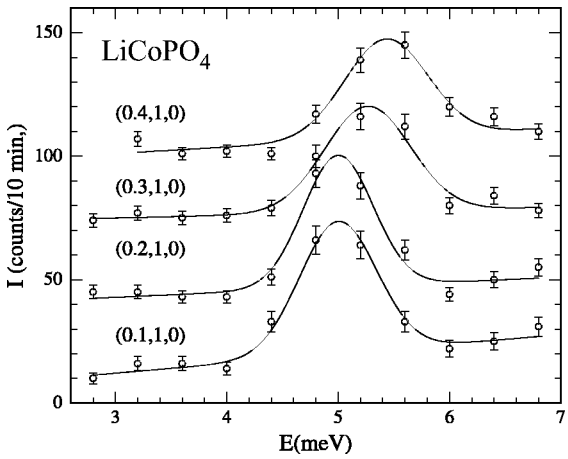

FIG. 5. Inelastic scattering at 10 K showing a slight dispersion along the $\xi_x=Q_xa/2\pi$. The absence of dispersion along the a axis demonstrates the quasi-2D character of the $LiCoPO_4$. It is argued that the observed resonance is due to the single-ion anisotropy (zero field splitting) term D.

Fitting the measured intensity in Fig. 3 with Eq. (4) yields $J_{2D}=-9.16\pm0.2$ K and $|\Delta_{G-E}|=0.064\pm0.01$ K.

Figure 4(a) shows inplane scans in the vicinity of the (210) Bragg reflection along the $(0k0)$ direction below and above the transition. The patterns consist of two superimposed peaks: a resolution-limited Bragg peak of the combined nuclear plus magnetic scattering, and a second broad peak due to the magnetic critical scattering. The analysis of the broad peak in terms of a Lorentzian line shape $1/(k^2+\kappa^2)$ yields κ which is inversely proportional to the coherence length ξ. The coherence length as a function of temperature is shown in Fig. 4(b) with a fit to the power law with a critical exponent $\nu=0.65$, which is very close to the theoretical value ($\nu\approx0.63$) of the 3D Ising model.[17] The solid line in Fig. 4 is the calculated coherence length of the 2D Ising model $\xi=a_{NN}[\ln\coth(J_{2D}/T-2J_{2D}/T]^{-1}$, where a_{NN} is the distance between nearest-neighbor spins in the plane.

2. Inelastic scattering

Inelastic scattering along the $(\xi00)$ and $(0\,\eta0)$ directions in the energy range 0–12 meV were performed around the (010) magnetic reflection. No in-plane spin waves were observed along the $(0\,\eta0)$ direction, which may be due to the large anisotropy gap requiring a higher-energy range. A prominent resonance with very little dispersion along the (100) direction was found at ≈5 meV, as shown in Fig. 5. We propose that the $E_g\approx5$ meV resonance is due to a single-ion anisotropy D (with a local term $-DS_z^2$ in the spin Hamiltonian), $D\approx E_g/2\approx29$ K. This excitation at 5 meV is also observed at temperatures well above T_N. The lack of dispersion in Fig. 5 is consistent with very weak interplane coupling.[19] Using the 2D integration mode, by removing the analyzer crystal to integrate over all 2D fluctuations,[18,20] we have not been able to observe any signal due to the spin dynamics, which are generally observed in Heisenberg-like

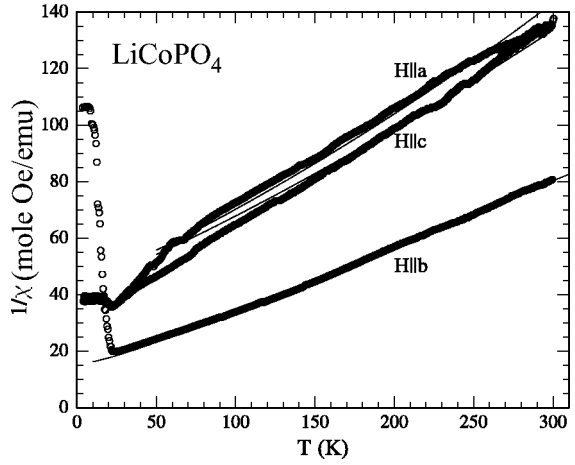

FIG. 6. Inverse magnetic susceptibility vs temperature of single crystal $LiCoPO_4$ measured along principal axial directions. The solid lines are calculated with a mean-field model that accounts for the single-ion anisotropy observed in the inelastic neutron scattering.

2D systems above or below T_N.[20] This is consistent with the prominent Ising-like behavior of this system (a pure Ising system cannot have propagating spin waves due to the discrete nature of the order parameter).

B. Magnetic susceptibility

The magnetic susceptibility versus temperature $\chi(T)$, of a $LiCoPO_4$ single crystal was reported recently,[9] and is reexamined here in view of the neutron-scattering studies. The inverse magnetic susceptibility $1/\chi(T)$ shown in Fig. 6 exhibits a strong anisotropy. Fitting the linear part in the temperature range 50 to 300 K, to the Curie-Weiss law $\chi(T)=C/(T+\theta)$, where $C=N_A(g\mu_B)^2S(S+1)/3k_B$, yields $\mu_{eff}(H\|b)=5.8\mu_B$ and $\mu_{eff}(H\|a)\approx\mu_{eff}(H\|c)=4.8\mu_B$.[9] $\Theta_a=-109$ K, $\Theta_b=-36$ K, and $\Theta_c=-81$ K. The fact that the value of the Curie temperature is lowest along the b axis is somewhat surprising since it indicates that the exchange along the b axis is the weakest and yet the moments at the AF phase are practically aligned along the b axis. We argue below that Curie temperature as extracted from the high-temperature susceptibility (the Curie-Weiss law) does not reflect the exchange interaction, as it can be affected artificially by the single-ion anisotropy that can give an artificial Curie temperature even in the absence of any exchange interaction.

To describe the susceptibility at high temperatures we use the molecular field (MF) approximation assuming the single ion-anisotropy term found in the neutron-scattering experiments. At high temperatures $T\gg J_\alpha$ ($\alpha=\|$ and $\perp$, respectively) the Hamiltonian in the MF approximation can be written as

$$\mathcal{H}=-g\mu_B[H_z^{eff}S_z+\tfrac{1}{2}(H_+^{eff}S_-+H_-^{eff}S_+)]+D(S_z^2-1/3S^2), \tag{5}$$

where $\mathbf{H}_\alpha^{eff}=\lambda_\alpha\mathbf{M}$ and $J_\alpha=\lambda_\alpha(g\mu_B)^2(N_A/V_A)/z$ (N_A is Avogadro's number and V_A is the volume) $\mathbf{M}$ is the magnetization, $z=4$ is the number of in-plane NN's, and $H_\pm=H_x\pm iH_y$, $S_\pm=S_x\pm iS_y$). In the MF approximation $\chi^\alpha(T)=\chi_0^\alpha/(1-\lambda\chi_0^\alpha)$, where χ_0^α is the free-spin susceptibility in the absence of exchange with the magnetic field parallel and perpendicular to the quantization axis. It is then calculated in the usual way,

$$\chi_0^\alpha(T)=\frac{N_A}{ZH_\alpha}\sum_i\frac{-dE_i^\alpha}{dH_\alpha}e^{-E_i^\alpha/T},$$

where Z is the partition function. The energy levels in the absence of exchange interaction ($\lambda=0$) E_i^α can be obtained by diagonalization of the 4×4 matrix associated with Eq. (5), in particular, for $H_\|$,

$$\begin{aligned}E^{(1,2)}&=-D\mp2X_\|,\\ E^{(3,4)}&=+D\mp3X_\|,\end{aligned} \tag{6}$$

and for $H_\perp$

$$\begin{aligned}E^{(1,2)}&=\pm X_\perp-\sqrt{D^2+4X_\perp^2-2X_\perp D},\\ E^{(3,4)}&=\pm X_\perp+\sqrt{D^2+4X_\perp^2-2X_\perp D},\end{aligned} \tag{7}$$

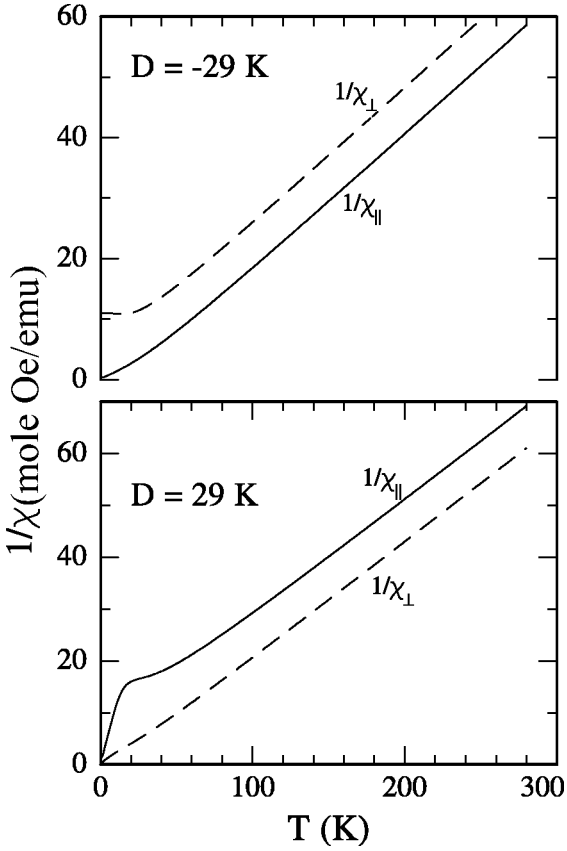

FIG. 7. Calculated inverse magnetic susceptibility vs temperature for a free $S=3/2$ paramagnetic system in the absence of exchange interaction, demonstrating the effect of the single-ion anisotropy. The high-temperature extrapolations yield a finite Curie temperature even though there is no exchange interaction.

where $X_\alpha \equiv g\mu_B H_\alpha$. Equations (6) and (7) show that at zero magnetic field the quartet is split into two doublets. The effect of the single ion anisotropy in the absence of exchange interactions, can be seen in Fig. 7. If D is negative, as suggested for $LiCoPO_4$, the inverse perpendicular susceptibility gives a finite Curie temperature, although the system is paramagnetic at all temperatures, as shown in Fig. 7. Using this procedure to fit the susceptibility in the temperature range 50–300 K with $D=-29$ K (as determined from the inelastic neutron scattering) yields $g=2.17\pm0.02$, $\lambda_\perp=33\pm3$, and $\lambda_\parallel=15\pm2$. The single-ion anisotropy D does not completely remedy the differences in the exchange anisotropy. The spin is along the b axis, whereas the exchange interaction is weakest along that direction. It is therefore suggested that the single-ion anisotropy determines the ground state of the spin system even though the exchange along that direction is smaller than in the other directions.

For the low-temperature region we examined the suitability of the 2D and 3D Ising models[21] in fitting the susceptibility data. A scale factor and the exchange, J_{2D} or J_{3D}, are the free parameters that are varied to give the best fits to the measured susceptibility at low temperatures. The parallel susceptibility $\chi_\parallel(T)$ for the square plane antiferromagnet was calculated by Sykes and Fisher (Ref. 22) using the series expansions method. Their calculation of $\chi_\parallel(T)$ is given in terms of two sets of series, one for $T \geqslant T_N$ [Eq. (5.18) of Ref. 22] and the other for $T \leqslant T_N$ [Eq. (6.7) Ref. 22]. The perpendicular susceptibility $\chi_\perp(T)$ corresponding to the plane square, was calculated exactly by Fisher.[23] The 2D square Ising model fits to the low-temperature data (using one scale factor and J_{2D} as free parameters) are shown as dashed lines in Figs. 8(a) and 8(b). These fits clearly suggest that the 2D square Ising model is insufficient to the description of the system. We have therefore also considered the 3D Ising model for the susceptibility at low temperatures. The solid line of the parallel susceptibility (Fig. 8) is based on series expansions calculations for the AF simple cubic Ising lattice by Fisher and Sykes.[24] The temperature dependence of the perpendicular susceptibility of the 3D Ising model (fcc lattice) given by Wang *et al.*[25] was used to fit the data in Fig. 8. Although the 3D models yield a better fit to the data, they are not adequate near the transition, and we ascribe this to the fact that the system is intermediate between the 2D and 3D systems.[26–28]

C. Magnetoelectric effect and symmetry

The linear magnetoelectric effect, characterized by the induction of a polarization P_k by a magnetic field H_i

$$P_k = \alpha_{ki} H_i \quad (\text{“ME}_H\text{ effect”}), \tag{8}$$

and of a magnetization M_k by an electric field E_i,

$$M_k = \alpha_{ik} E_i \quad (\text{“ME}_E\text{ effect”}), \tag{9}$$

is allowed in 19 ferromagnetic point groups and 39 antiferromagnetic ones.[29] By determining the nonzero components of the α_{ki} tensor the magnetic point group and the magnetic space group—if the nuclear structure is known—can in principle be determined.[30,31] This has been done for the four

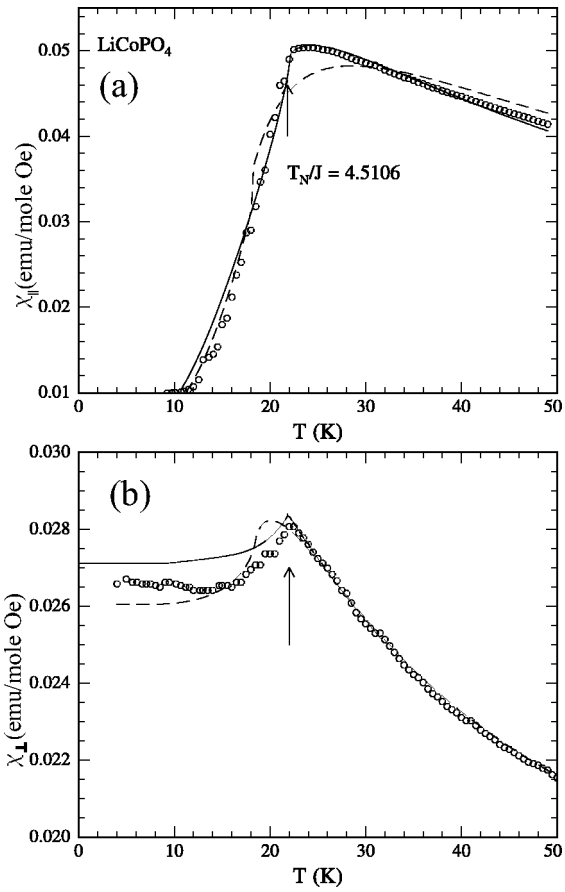

FIG. 8. (a) Parallel and (b) perpendicular magnetic susceptibilities vs temperature around the AF transition temperature. The solid and dashed lines in (a) are calculated by the series expansion for the simple cubic and square Ising systems, respectively, as given in Refs. 22 and 24. The solid line in (b) the calculated perpendicular susceptibility for the fcc Ising system as given by Wang *et al.* (Ref. 25). The dashed line in (b) is the calculated perpendicular susceptibility for square Ising system as given by Fisher (Ref. 23).

lithium orthophosphates $LiMPO_4$ (M=Mn, Fe, Co, Ni) by Mercier.[32,33] For $LiCoPO_4$ the nonzero components α_{xy} and α_{yx} of the ME susceptibility tensor were found, corresponding to the orthorhombic point and space group mmm' and $Pnma'$, respectively, consistent with neutron diffraction results.[3] The temperature dependences of α_{xy} and α_{yx} were found to be in good agreement with the ‘‘single-ion’’ and ‘‘two-ion’’ theories.[32] More recently more accurate quasistatic and dynamic $(ME)_H$ effect measurements have been performed on $LiCoPO_4$,[8] confirming that no other tensor components than the coefficients α_{xy} and α_{yx} were measurable. However, some new features have been disclosed: (i) Magnetic single domains (or ‘‘partial’’ single domains, see below) have been produced by cooling in a magnetic field *alone*, applied along the b axis.[8] Since fully compensated ME antiferromagnets can only be rendered single domain by *simultaneously* applying a magnetic field and an electric field,[34,35] this observation suggests the existence of a spontaneous magnetization along the b axis. (ii) ME ‘‘butterfly’’ loops have been observed closely below the Néel temperature, by applying and reversing by 180° a magnetic field

along the *b* axis (i.e., the spin direction), as well as by rotating a constant magnetic field in the orthorhombic *b*-*c* plane.[8] The measurement of butterfly loops for the magnetic field along the *b* axis has also been extended to lower temperatures and to higher fields.[36] Magnetoelectric butterfly loops are known to be the signature of a spontaneous magnetization. Several examples are known in the crystal family of the weakly ferromagnetic/ferroelectric/ferroelastic boracites.[37–40] (iii) The occurrence of magnetoelectric butterfly loops has also been theoretically predicted for the case of ''hidden weak ferromagnetism'' (i.e., of mutually compensating ''weakly ferromagnetic'' sublattices).[41] However, the observed presence of a spontaneous magnetization [(see (iii)] rules out this explanation for $LiCoPO_4$. (iv) It was shown by phenomenological theory[42] that the butterfly loop can also be explained by the inclusion of an incommensurate magnetic modulation. However, the present neutron diffraction study did not show any incommensurate structure. Thus this type of mechanism is also ruled out. (v) Recent measurements by means of a superconducting quantum interference device have clearly confirmed the existence of a very weak spontaneous magnetization along the *b* axis of $LiCoPO_4$.[43] This means that the compound has a symmetry lower than that of the so-far-admitted fully compensated antiferromagnetic structure with point group $m_x m_y m_z'$ (magnetic space group $Pnma'$). For the true lower symmetry one can claim that its tensor components of the linear ME effect must be identical to those of point group $m_x m_y m_z'$ or contain the coefficients α_{xy} and α_{yx} in addition to other components. The orthorhombic point groups with identical tensor form of the magnetoelectric susceptibility $[\alpha_{ki}]$ [cf. Eq. (8) and Ref. 44] are the following:

$$2_x' 2_y' 2_z, \quad m_x m_y 2_z, \quad 2_x' m_y m_z', \quad m_x 2_y' m_z', \quad m_x m_y m_z',$$

$$[\alpha_{ki}] = \begin{bmatrix} \cdot & \bullet & \cdot \\ \bullet & \cdot & \cdot \\ \cdot & \cdot & \cdot \end{bmatrix}, \quad \text{first setting} \tag{10}$$

(large dots indicate nonvanishing tensor elements). One can see that the polar group $2_x' m_y m_z'$ is the only orthorhombic one-permitting a spontaneous magnetization along the y-axis. However, in the present study a rotation of the spin direction of about 4.6° from the *b* axis within the *bc* plane has been observed. This means that the mirror m_y and the anti-mirror m_z' have in fact been lost, implying a symmetry lower than orthorhombic.

From Fig. 2 of Ref. 44 we see that the tensor forms of the linear ME effect for the crystallographic ''first setting'' (monoclinic principal axis along the *z* axis) and the ''second setting'' (monoclinic principal axis parallel to *y* axis) are not compatible with a magnetization parallel to the *y* axis except for point group m_y:

$$2_y', \quad m_y, \quad 2_y'/m_y;$$

$$[\alpha_{ki}] = \begin{bmatrix} \cdot & \bullet & \cdot \\ \bullet & \cdot & \bullet \\ \cdot & \bullet & \cdot \end{bmatrix}, \quad \text{second setting.} \tag{11}$$

However, the mirror m_y having been lost, group m_y has to be discarded. Thus we have to examine also the ''third-setting'' (the monoclinic principal axis parallel to *x*), which is normally not used in crystallography, but for which we find the following potential groups and tensor forms:

$$2_x, \quad m_x', \quad 2_x/m_x';$$

$$[\alpha_{ki}] = \begin{bmatrix} \bullet & \cdot & \cdot \\ \cdot & \bullet & \bullet \\ \cdot & \bullet & \bullet \end{bmatrix}, \quad \text{third setting,} \tag{12}$$

$$2_x', \quad m_x', \quad 2_x/m_x';$$

$$[\alpha_{ki}] = \begin{bmatrix} \cdot & \bullet & \bullet \\ \bullet & \cdot & \cdot \\ \bullet & \cdot & \cdot \end{bmatrix}, \quad \text{third setting.} \tag{13}$$

From Eqs. (12) and (13) it becomes clear that group $2_x'$ is the only possible one since its tensor contains α_{xy} and α_{yx} and the spontaneous magnetization being allowed in a direction in the *yz* plane perpendicular to the $2_x'$ axis,[45] including the experimentally observed spontaneous magnetization along the *b* axis.[43] Groups $2_x/m_x'$ and $2_x'/m_x$ being antiferromagnetic, they have to be discarded. It is noteworthy that $2_x'$ is also ferrotoroidic,[46] i.e., allowing a spontaneous toroidal moment in a direction lying in the pseudo-orthorhombic *yz* plane.[46,47,50] If we want to describe group $2_x'$ (where *x* is a pseudo-orthorhombic index) in terms of the usually used monoclinic ''second-setting'' standard form $2_{y(m)}'$, the pseudo-orthorhombic *x* axis becomes the monoclinic principal axis $y(m)$, i.e., $x \rightarrow y(m)$, $y \rightarrow x(m)$ and $z \rightarrow z(m)$, and the ''second setting'' standard form of the tensor $\alpha_{ik(m)}$ takes the above mentioned form [Eq. (11)]. This means, however, that the measured pseudo-orthorhombic α_{xy} and α_{yx} (Ref. 3) become the measured monoclinic $\alpha_{yx(m)}$ and $\alpha_{xy(m)}$, respectively. The experimental nonobservation of the coefficients $\alpha_{yz(m)}$ and $\alpha_{zy(m)}$ is plausible, since the 4.6° rotation of the spins from the *b*-axis direction represents only a very small deviation from the symmetry of point group $2_x' m_y m_z'$. The monoclinic magnetic space group is $P2_1'11$ (point group $2_x'$) if the pseudo-orthorhombic *a* axis is taken as unique axis or $P12_1'1$ (point group $2_{y(m)}'$) if the monoclinic *b* axis is considered as unique axis. Point group $2_{y(m)}$' is also consistent with the observation of the linear magneto-optic effect[48] in LiCoPO4,[49] which is possible in the 66 magnetic point groups allowing piezomagnetism (Table II of Ref. 29), but which is not permitted in the initially assumed group $m_x m_y m_z'$.

D. Multiferroic properties

The Shubnikov-Heesch point group 2' belongs to an ensemble of nine point groups, allowing in the same phase a spontaneous polarization (for $2'$ along the $2'$ axis), a spontaneous magnetization and a spontaneous toroidal moment (for $2'$ in arbitrary directions in the x-z plane, i.e., perpendicular to the $2'$ axis) [Ref. 50 (here current density stands for toroidal moment), Ref. 45 (Table I, for spontaneous magnetization and polarization)]. The potential existence of a ferroelectric polarization along the $2_{y(m)}$'-axis of $LiCoPO_4$ has so far not yet been measured. Since the orthorhombic $\rightarrow$monoclinic phase transition is essentially due to spin ordering and not to important ionic shifts, one can expect only an extremely small reversible spontaneous polarization (a kind of ''electronic ferroelectricity''). For a given fixed experimental coordinate system the sign of the magnetoelectric coefficients will not be influenced by the 180° reversal of spontaneous polarization (due to invariance of the spin system under space inversion).

1. Possible domain states

The phase transition from the paramagnetic orthorhombic phase of Shubnikov point group $mmm1'$ to the monoclinic ferroic phase and the twinning of the latter one is described by ''Aizu species'' $mmm1'F2'$,[51] resulting in two possible ferroelastic domains with opposite shear components in the a_m-c_m plane and two possible ferroelectric 180° domains inside each of the two ferroelastic domains with the spontaneous polarization parallel to the monoclinic b axis (equal to the pseudo-orthorhombic a axis). Inside each ferroelectric/ferroelastic domain two 180° ferromagnetic domains are possible, with their spontaneous magnetization in an arbitrary direction within the monoclinic $(010)_m$ plane.[45] The experiment shows that said magnetization lies parallel or very close to the monoclinic $\langle 010\rangle_m$ direction (equal to the orthorhombic $\langle 100\rangle$ direction). Thus a total of $2\times2\times2=8$ domain states is in principle possible. The classification according to Aizu of species $mmm1'F2'$ is denominated: *partially ferromagnetic, partially ferroelastic and partially ferroelectric* (see Ref. 51; in Ref. 52 *Ensemble No.* 14 of Table I). This simply means that neither an electric field alone, a magnetic field alone nor stress alone and electric plus magnetic fields alone are able to produce a *ferroelectric/ferromagnetic/ferroelastic* single domain. The two ferroelastic domain states should be characterized by an opposite 4.6° rotation of the spins over the monoclinic b axis and the two ferromagnetic domains inside one of the two ferroelastic domains should consequently have the same sense of the 4.6° rotation of the spins. Ferroelastic domains can in principle be made visible by polarized light techniques; however, attempts at observing such domains with nearly crossed polarizers perpendicular to the a_m-c_m plane remained unsuccessful.[53] This is further evidence that the deviation from the orthorhombic symmetry must be extremely small. The degeneracy of ferroelastic domains can in principle be lifted by appropriately applied stress; however, the monoclinic angle β being apparently equal to zero, the lifting of the degeneracy by stress will in practice not be possible. Although the above mentioned [C./(i)] cooling in a magnetic field along the orthorhombic b axis aligned the ferromagnetic domains, they may have been ferroelectrically and ferroelastically degenerate because of their so called partially ferromagnetic character. An efficient alternate method for observing antiferromagnetic domains, as well as ferromagnetic domains would be *topography* based on magnetic second harmonic generation. (see, e.g., Refs. 54 and 55). Since this method is not only sensitive to time-reversal-related domains but also to the spin direction, the postulated ferroelastic domains with opposite 4.6° rotation of the spins over the orthorhombic a axis might be made visible by that method. Stress-free ferroelastic domain walls of species $mmm1'F2'$ may run along the lost orthorhombic mirror planes m_y and/or m_z.[56]

2. Weak spontaneous magnetic moment

Group $2'_y$ allows weak ferromagnetism (see Table 2 of Ref. 29). According to Tavger[57] a classical weak ferromagnetic moment in antiferromagnets can only occur perpendicularly to the antiferromagnetic spin direction. However, this is not the case for $LiCoPO_4$ since the direction of spontaneous magnetization is roughly parallel to the spin direction. Thus the phenomenology might be described as a ''very weak ferrimagnetism.'' More theoretical work is necessary for understanding this behavior.

IV. CONCLUSIONS

The temperature dependence of the AF order parameter in single crystal $LiCoPO_4$ has been determined from neutron-scattering experiments. It has been shown that the spins are slightly rotated from the principal b axis. Such a rotation of the spins requires the symmetry to be lower than the point group mmm' (space group $Pmna'$). The analysis of the magnetic susceptibility was reexamined in order to explain the unique anisotropy in this system. Whereas the Curie-Weiss law analysis suggests that the exchange along the b axis is weaker than in the other two perpendicular directions, the spins in the ground state align along the b axis. We have shown that extracting exchange interaction strength from the Curie temperature can be misleading when the spin Hamiltonian contains a single ion anisotropy term. By combining the results (i) of neutron diffraction (in particular the 4.6° rotation of the spins over the orthorhombic a axis), (ii) of the measurement of the linear magnetoelectric effect, and (iii) the measurement of a spontaneous magnetization along the orthorhombic b axis, one has to admit a decrease in symmetry from the hitherto admitted orthorhombic antiferromagnetic point group mmm' (space group $Pnma'$) to monoclinic symmetry with magnetic point group $2'$ (magnetic space group $P2'_111$) if the pseudo-orthorhombic a axis is taken as unique axis or $P12'_11$ if the monoclinic b axis is taken as the unique axis. As mentioned above, the magnetic structure model adopted in this paper is not unique. Therefore more experimental and theoretical work is necessary to confirm the true magnetic symmetry of $LiCoPO_4$.

ACKNOWLEDGMENTS

D.V. and J.L.Z. thank the Solid State Division at Oak Ridge National Laboratory for the technical support extended during the neutron scattering experiments. Ames Laboratory is operated for the U.S. Department of Energy by Iowa State University under Contract No. W-7405-Eng-82. The work at Ames was supported by the Director for Energy Research, Office of Basic Energy Sciences. Thanks are due to Professor E. Parthé (Geneva) for discussions on symmetry, and to Professor M. Mercier (Montulçon) for providing the single crystal.

[1] J. M. Mays, Phys. Rev. **131**, 38 (1963).
[2] R. P. Santoro, R. E. Newnham, and S. Nomura, J. Phys. Chem. Solids **27**, 655 (1966).
[3] R. P. Santoro, D. J. Segal, and R. E. Newnham, J. Phys. Chem. Solids **27**, 1192 (1966).
[4] R. P. Santoro and R.E. Newnham, Acta Crystallogr. **22**, 344 (1967).
[5] J. L. Z. Zarestky, D. Vaknin, B. C. Chakoumakos, T. Rojo, A. Goñi, and G. E. Barberis, J. Magn. Magn. Mater. **234**, 401 (2001).
[6] H. D. Megaw, *Crystal Structures—A Working Approach* (Saunders, Philadelphia, 1973), p. 249.
[7] A. Goñi, T. J. Bonagamba, M. A. Silva, H. Panepucci, T. Rojo, and G. E. Barberis, J. Appl. Phys. **84**, 416 (1998); A. Goñi, L. Lezama, G. E. Barberis, J. L. Pizarro, M. I. Arriortua, and T. Rojo, J. Magn. Magn. Mater. **164**, 251 (1996); A. Goñi, J. L. Pizarro, L. M. Lezama, G. E. Barberis, M. I. Arriortua, and T. Rojo, J. Mater. Chem. **6**, 412 (1996).
[8] J.-P. Rivera, Ferroelectrics **161**, 147 (1994); J.-P. Rivera and H. Schmid, *ibid.* **161**, 91 (1994).
[9] J.-P. Rivera, J. Korean Phys. Soc. **32**, S1855 (1998).
[10] F. Kubel, Z. Kristallogr. **209**, 755 (1994).
[11] L. Onsager, Phys. Rev. **65**, 117 (1944); C. N. Yang, *ibid.* **85**, 809 (1952).
[12] J. W. Essam and M. E. Fisher, J. Phys. Chem. **38**, 802 (1963).
[13] L. J. de Jongh, in *Magnetic Properties of Layered Transition Metal Compounds*, edited by L. J. de Jongh (Kluwer, Dordrecht 1990), p 1.
[14] A. Abragam and B. Bleaney, *Electron Paramagnetic Resonance of Transition Metals* (Clarendon Press, Oxford, 1970), pp. 363–471.
[15] M. Plischke and B. Bergersen, *Equilibrium Statistical Physics* (Prentice Hall, Englewood Cliffs, NJ, 1989).
[16] K. Hirakawa and H. Ikeda in *Magnetic Properties of Layered Transition Metal Compounds* (Ref. 13), p. 271.
[17] A. M. Ferrenberg and D. P. Landau, Phys. Rev. B **44**, 5081 (1991).
[18] B. J. Birgeneau, J. Als-Nielsen, and G. Shirane, Phys. Rev. B **16**, 280 (1977).
[19] A. F. M. Arts and H. W. De Wijn, in *Magnetic Properties of Layered Transition Metal Compounds* (Ref. 13), p. 191.
[20] D. Vaknin, L. L. Miller, J. L. Zarestky, and D. C. Johnston, Physica C **274**, 331 (1997).
[21] M. E. Fisher, Rep. Prog. Phys. **30**, 615 (1967).
[22] M. F. Sykes and M. E. Fisher, Physica (Amsterdam) **28**, 919 (1962).
[23] M. E. Fisher, J. Math. Phys. **4**, 125 (1963).
[24] M. E. Fisher and M. F. Sykes, Physica (Amsterdam) **28**, 939 (1962).
[25] Y. L. Wang, C. Wentworth, and B. Westwanski, Phys. Rev. B **32**, 1805 (1985).
[26] D. J. Breed, K. Gilijamse, and A. R. Miedema, Physica (Amsterdam) **45**, 205 (1969).
[27] E. J. Samuelson, Phys. Rev. Lett. **31**, 936 (1973).
[28] H. Ikeda and K. Hirakawa, Solid State Commun. **14**, 529 (1974).
[29] H. Schmid, Int. J. Magn. **4**, 337 (1973); and in *Magnetoelectric Interaction Phenomena in Crystals*, edited by A.J. Freeman and H. Schmid (Gordon and Breach, London, 1975).
[30] *Proceedings of the Second International Conference on Magnetoelectric Interaction Phenomena in Crystals (MEIPIC-2), Ascona, 1993, Parts I and II*, edited by Hans Schmid, Aloysio Janner, Hans Grimmer, Jean-Pierre Rivera, and Zuo-Guang Ye [Ferroelectrics **161**, 1 (1994); **162**, 1 (1994)].
[31] Hans Schmid, Proc. SPIE **4097**, 12 (2000).
[32] M. Mercier, Thèse de doctorat d'Etat, Faculté des Sciences, Université de Grenoble, France, 1969.
[33] M. Mercier, Rev. Gen. Electr. **80**, 143 (1971).
[34] T. J. Martin, Phys. Lett. **17**, 83 (1965).
[35] T. J. Martin and C. J. Anderson, IEEE Trans. Magn. **MAG-2**, 466 (1966).
[36] H. Wiegelmann, Ph.D. thesis, University of Konstanz, 1995 (Konstanzer Dissertationen, Bd. 461, Hartung-Gorre, Konstanz, 1995).
[37] E. Ascher, H. Rieder, H. Schmid, and H. Stössel, J. Appl. Phys. **37**, 1404 (1966).
[38] J.- P. Rivera, H. Schmid, J. M. Moret, and H. Bill, Int. J. Magn. **6**, 221 (1974).
[39] J.-P. Rivera and H. Schmid, Ferroelectrics **55**, 295 (1984).
[40] M. Senthil Kumar, J.-P. Rivera, Z. G. Ye, S. D. Gentil, and H. Schmid, Ferroelectrics **204**, 57 (1997).
[41] I. E. Chupis, Low Temp. Phys. **26**, 419 (2000).
[42] I. Kornev, M. Bichurin, J.-P. Rivera, S. Gentil, H. Schmid, A. G. M. Jansen, and P. Wyder, Phys. Rev. B **62**, 12 247 (2000).
[43] N. F. Kharchenko, Yu. N. Kharchenko, R. Szymczak, M. Baran, and H. Schmid, Low Temp. Phys. **27**, 895 (2001).
[44] J.-P. Rivera, Ferroelectrics **161**, 165 (1994).
[45] E. Ascher, J. Phys. Soc. Jpn. **28**, Suppl., 7 (1970).
[46] H. Schmid, Ferroelectrics **252**, 41 (2001).
[47] E. Ascher, Helv. Phys. Acta **39**, 40 (1966).
[48] N. F. Kharchenko, Ferroelectrics **162**, 173 (1994).
[49] N. F. Kharchenko, O. V. Myloslavska, Y. M. Kharchenko, H. Schmid, and J. P. Rivera, Ukr. J. Phys. Opt. **1**, 16 (2000).
[50] E. Ascher, Helv. Phys. Acta **39**, 40 (1966).
[51] K. Aizu, Phys. Rev. B **2**, 757 (1970).
[52] H. Schmid, Ferroelectrics **221**, 9 (1999).

[53] J.-P. Rivera (unpublished).
[54] St. Leute, Th. Lottermoser, and D. Fröhlich, Opt. Lett. **24**, 1520 (1999).
[55] D. Fröhlich, Th. Kiefer, St. Leute, and Th. Lottermoser, Appl. Phys. B: Lasers Opt. **68**, 465 (1999).
[56] J. Sapriel, Phys. Rev. B **12**, 5128 (1975).
[57] B. A. Tavger, Kristallografiya **3**, 339 (1958) [Sov. Phys. Crystallogr. **3**, 341 (1958)].